



## Determining the quantum-coherent to semiclassical transition in atomic-scale quasi-one-dimensional metals

Bent Weber<sup>1,2,\*</sup> and Michelle Y. Simmons<sup>1,†</sup>

<sup>1</sup>*Centre of Excellence for Quantum Computation and Communication Technology, School of Physics, University of New South Wales, Sydney, New South Wales 2052, Australia*

<sup>2</sup>*School of Physics & Astronomy, Monash University, Clayton, Victoria 3800, Australia*

(Received 5 July 2016; published 29 August 2016)

Atomic-scale silicon wires, patterned by scanning tunneling microscopy (STM) and degenerately doped with phosphorus (P), have attracted significant interest owing to their exceptionally low resistivity and semiclassical Ohmic conduction at temperatures as low as  $T = 4.2$  K. Here, we investigate the transition from semiclassical diffusive to quantum-coherent conduction in a 4.6 nm wide wire as we decrease the measurement temperature. By analyzing the temperature dependence of universal conductance fluctuations (UCFs) and one-dimensional (1D) weak localization (WL)—fundamental manifestations of quantum-coherent transport in quasi-1D metals—we show that transport evolves from quantum coherent to semiclassical at  $T \sim 4$  K. Remarkably, our study confirms that universal concepts of mesoscopic physics such as UCF and 1D WL retain their validity in quasi-1D metallic conductors down to the atomic scale.

DOI: [10.1103/PhysRevB.94.081412](https://doi.org/10.1103/PhysRevB.94.081412)

Individual phosphorus (P) donors, precision placed within the silicon crystal by scanning tunneling microscopy (STM) [1–4], are attracting growing interest as candidates for quantum bits (qubits) in solid-state quantum information processing. However, the engineering of scalable quantum computing architectures [5–7] will rely on forming arrays of exchange-coupled donor qubits with atomic-precision alignment of gate electrodes and electron reservoirs at a similar length scale as the P donor atoms themselves (Bohr radius  $a_B \simeq 2.5$  nm). We have recently shown that electrodes of such extreme dimensions can be patterned by STM [2,8] and exhibit semiclassical Ohmic conduction with exceptionally low resistivity at temperatures down to  $T = 4.2$  K. This has since allowed the implementation of these electrodes within increasingly complex device architectures [4,9–11] for Si:P donor-based quantum information processing.

The semiclassical metallic attributes of these Si:P wires seem surprising [12], regarding that these atomic-scale electronic systems have been measured at cryogenic temperatures (4.2 K) where quantum effects can be expected to dominate. In particular, here the quantum phase-coherent nature of the conduction electrons in a disorder potential is expected to localize electronic wave functions, leading to insulating behavior [13]. In a recent communication [8] we have indeed shown that metallic conduction in STM-patterned Si:P wires is fundamentally limited by a metal-insulator transition driven by Anderson localization [13–15]. While electron transport in the metallic regime remains well described by semiclassical Drude models at  $T = 4.2$  K [8,16], conductance fluctuations with a Gaussian distribution and root mean square amplitude  $\delta G_W \sim e^2/h$  [8] emerge at millikelvin temperatures, consistent with universal conductance fluctuations (UCFs) [17–19]—a fundamental manifestation of phase-coherent diffusive conduction in quasi-one-dimensional (quasi-1D) metals. In this Rapid Communication, we explore the limits of phase-coherent

transport by analyzing UCFs in the presence of magnetic and gate-induced electric fields. This allows us to obtain estimates of the length scale over which electron phase coherence is maintained—the phase-coherence length  $l_\varphi$ . Importantly, we determine the transition from the quantum phase-coherent to semiclassical regime at a temperature  $T = 4.2$  K [2,8], and confirm that these fundamental concepts of mesoscopic physics remain valid in quasi-1D metallic conductors at the atomic scale.

A 47 nm long silicon wire as narrow as 4.6 nm is shown in Figs. 1(a) and 1(b). This wire was patterned by scanning tunneling microscopy (STM) lithography on the hydrogen terminated Si(001)- $2 \times 1$  reconstructed surfaces of  $n$ -doped (P, 1–10 m $\Omega$ cm) substrates [2,8]. An atomic-resolution STM image of the wire is shown in Fig. 1(b), showing the atomic dimer rows of the Si(001)- $2 \times 1$  surface reconstruction. Following lithography, the wire was exposed to phosphine (PH<sub>3</sub>) gas ( $5 \times 10^{-8}$  mbar, 6 min), passivating the reactive silicon dangling bonds. This protects the wire against contaminants during patterning of larger electrodes ( $S, D, V_1, V_2$ ) and gates ( $G1, G2$ ) which connect the wire to micrometer-scale Si:P-doped contacts [2,8]. As previously shown [8], two electrodes on either end of the wire allow four-probe measurements, providing a precise measure of the wire conductance independent of contact resistances [20]. A second exposure to PH<sub>3</sub>, followed by annealing (350 °C, 1 min), and low-temperature (250 °C, 3 h) silicon epitaxy ( $\simeq 25$  nm), selectively dopes the completed pattern to 1/4 monolayer planar density ( $N_{2D} \simeq 2 \times 10^{14}$  cm<sup>2</sup>) [21,22] with atomically sharp doping profiles. The equivalent bulk density  $N_{3D} \sim 10^{21}$  cm<sup>3</sup> is three orders of magnitude higher than the critical density ( $\simeq 3 \times 10^{18}$  cm<sup>3</sup>) of the Mott metal-insulator transition [23], providing a highly metallic electron system [2].

Electron transport was measured in a <sup>3</sup>He/<sup>4</sup>He dilution refrigerator with a base temperature of  $\sim 50$  mK (electron temperature  $\simeq 200$  mK). The sample was mounted with the magnetic field applied perpendicular to the Si:P  $\delta$ -doped plane. Four-probe electrical characterizations were subsequently

\*bent.weber@gmx.de

†michelle.simmons@unsw.edu.au

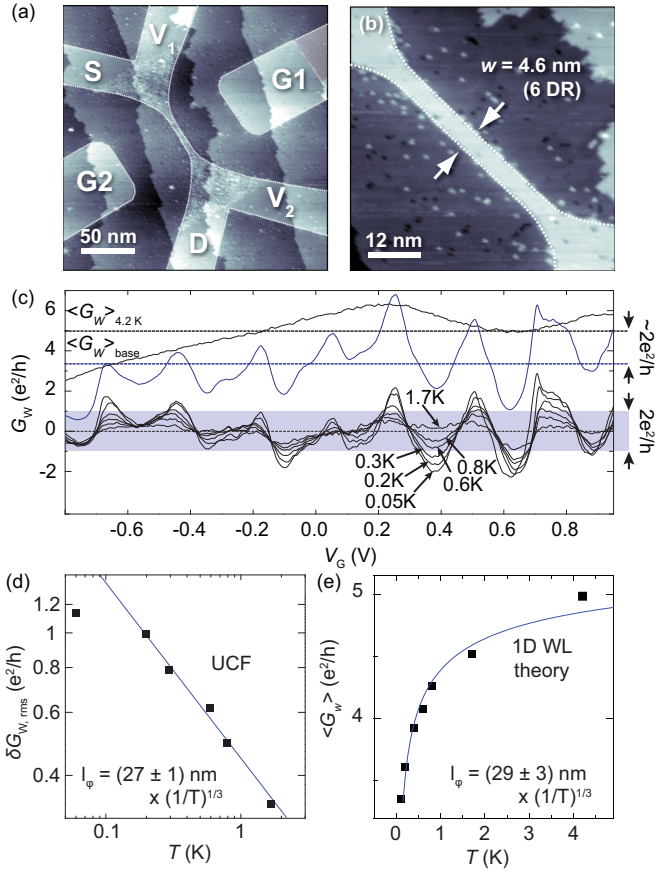


FIG. 1. Phase-coherent transport in a 4.6 nm wide silicon nanowire. (a) Overview STM image of a 4.6 nm wide and 47 nm long nanowire after STM hydrogen lithography. (b) High-resolution STM image of the wire showing its precise lithographic width corresponding to six dimer rows (DR) of the Si(001)- $2 \times 1$  surface reconstruction. (c) Temperature dependence of the measured four-terminal conductance and conductance fluctuations of order  $\sim e^2/h$ . Horizontal lines indicate the calculated mean conductance  $\langle G_W \rangle$  used for the background subtraction (see main text). (d) Root mean square amplitude  $\delta G_{W,rms}$  of the conductance fluctuations as a function of temperature. (e) Mean conductance  $\langle G_W \rangle$  as a function of temperature. Both (d) and (e) have been extracted from (c) (see main text).

performed using standard dc measurement techniques with gate voltages applied simultaneously to  $G1$  and  $G2$ .

A comparison of the conductance  $G_W$  measured at  $T = 4.2$  K (black) and at the base temperature ( $T_{el} \simeq 200$  mK) of our dilution refrigerator (blue) [8] is shown in Fig. 1(c). In these data, electron phase coherence manifests itself twofold [19,24,25]. First, as we reduce temperature, weak localization (WL) causes an overall reduction  $\delta G_{WL} \sim 2e^2/h$  of the mean conductance  $\langle G_W \rangle$  (dashed horizontal lines), consistent with 1D weak localization [19]. Second, at 200 mK we observe fluctuations with an amplitude  $\delta G_W \sim e^2/h$  around the mean conductance (blue shaded band), consistent with UCF. Both phenomena arise from quantum interference of diffusively propagating carriers along quasi-1D metals [19], and can be described based on their well-known dependencies on temperature  $T$  and applied magnetic field  $B$ .

The conductance fluctuations after correcting for both temperature- and gate-voltage-dependent backgrounds are plotted in Fig. 1(c) (bottom) and are seen to collapse around  $G_W = 0$ . For this background correction, we first subtract the mean conductance ( $G_W$ ) at each measurement temperature, followed by a subtraction of the conductance measured at  $T = 4.2$  K, corrected by its mean. This now allows for a statistical analysis of the fluctuations. The root mean square (rms) amplitude of the fluctuations is plotted in Fig. 1(d). The saturation below  $T \lesssim 200$  mK occurs as the electron temperature exceeds the mixing chamber temperature of our dilution refrigerator. The temperature-dependent mean conductance used for the background subtraction is plotted in Fig. 1(e). In these figures, solid blue lines show fits to the Lee, Stone, and Fukuyama theory of UCF [18,19,26] and 1D WL [19,27], respectively, providing two independent methods to extract the phase-coherence length  $l_\phi$ .

The observed power law temperature dependence of the fluctuations in the low-temperature limit ( $l_\phi \ll l_T$  where  $l_T = \sqrt{\hbar D/k_B T}$  [28]) is described by

$$\delta G_{UCF} = \alpha C \frac{g_s g_v}{2} \beta^{-1/2} \left( \frac{e^2}{h} \right) \left( \frac{l_\phi}{L} \right)^{3/2}. \quad (1)$$

Here,  $C$  is a constant of order unity [18,26]. The factor  $\beta = 1, 2$  describes the symmetry of the system, where  $\beta = 1$  for time-reversal symmetry, and  $\beta = 2$  otherwise. The factor  $\alpha = \{1, \dots, 1/g_v\}$  is a measure of the intervalley scattering strength [29], where  $g_v = 6$  is the valley degeneracy of P  $\delta$ -doped silicon [8,30].

The temperature dependence enters Eq (1) implicitly, as the phase-coherence length follows a power law temperature dependence  $l_\phi \propto (1/T)^p$ , where  $p$  is determined by the dominant phase-breaking mechanism. From the fit in Fig. 1(d), we find

$$\delta G_{W,rms} = (0.45 \pm 0.02) \left( \frac{1}{T} \right)^{(0.49 \pm 0.03)} \quad (2)$$

in units of  $e^2/h$ , from which we extract

$$l_\phi = (27 \pm 1) \left( \frac{1}{T} \right)^{(0.33 \pm 0.02)} \text{ nm}. \quad (3)$$

For this estimate, we have assumed  $\beta = 1$ , as well as  $C = 1$  [31,32], and  $\alpha g_v = 1$  for strong intervalley scattering [33].

The only dephasing mechanism known with a temperature exponent  $p = 1/3$  is electron-electron scattering with small energy transfers—the so-called Nyquist dephasing—which can be understood as scattering of carriers with the fluctuating electric field generated by the quasi-1D electron gas [34]. Nyquist scattering has been found to universally dominate dephasing at low temperature, in a wide variety of quasi-1D metallic systems, ranging from metal wires [35–37] to carbon nanotubes [38] and quasi-1D semiconductor nanostructures such as silicon metal-oxide-semiconductor field-effect transistors (MOSFETs) [39,40] and larger delta-doped silicon wires [41]. We can compare the extracted phase-coherence length with that which is theoretically predicted for quasi-1D

disordered metals [42],

$$l_\varphi = \left( \frac{D\hbar^2 L G_0}{\sqrt{2}e^2 k_B T} \right)^{1/3} = 69 \left( \frac{1}{T} \right)^{1/3} \text{ nm}, \quad (4)$$

and find reasonable agreement within a factor of 2. For this estimate, we used the diffusion constant,  $D = 1/2v_F l = 1.8 \times 10^{-3} \text{ cm}^2/\text{s}$ , where  $v_F = \hbar k_F/m^*$ , with  $m^* = 0.28m_e$ ,  $k_F = \sqrt{4\pi n_s/g_s g_v} = 1.45 \text{ nm}^{-1}$ , and an electron mean free path  $l = 6 \text{ nm}$  [8].  $G_0$  is the semiclassical Drude conductance for which we assume  $G_W = 4.7e^2/h$ , measured at  $T = 4.2 \text{ K}$  and at  $V_G = 0 \text{ V}$ .

To confirm this estimate of the phase-coherence length, we also fit the temperature-dependent mean conductance [Fig. 1(e)] with a sum of the (temperature-independent) Drude conductance  $G_0$  [8] and a (temperature-dependent) 1D weak localization correction  $\delta G_{WL}(T)$  [19,27],

$$\langle G_W \rangle(T) = G_0 + \delta G_{WL}(T), \quad (5)$$

where [42,43]

$$\delta G_{WL} = -g_s g_v \frac{e^2}{h} \left( \frac{l_\varphi}{L} \right). \quad (6)$$

Assuming Nyquist dephasing ( $p = 1/3$ ) and  $\alpha_{g_v} = 1$ , we find

$$l_\varphi = (29 \pm 3) \left( \frac{1}{T} \right)^{0.33} \text{ nm}, \quad (7)$$

in excellent agreement with the value extracted from the UCF temperature dependence. Remarkably, this estimate agrees exceptionally well with much wider ( $w > 30 \text{ nm}$ ) STM-patterned wires [41] where  $l_\varphi = 40 \times (1/T)^{0.31} \text{ nm}$  was found by analysis of 1D weak localization.

Consistent values of the coherence length extracted from two separate (though related) theories thus corroborates the presence of quasi-1D diffusive quantum transport in these atomic-scale metals. The extracted temperature dependence  $l_\varphi \simeq 28 \text{ nm} \times (1/T)^{1/3}$  now allows us to extrapolate the coherence length at  $T_e \simeq 200 \text{ mK}$ , where we find  $l_\varphi = (48 \pm 3) \text{ nm}$ . Notably, this value closely coincides with the wire length,  $L = 47 \text{ nm}$ , implying that transport is fully phase coherent ( $l_\varphi \approx L$ ). Indeed, at this temperature, the conductance fluctuations reach their universal amplitude,  $\delta G_{W,rms} \sim e^2/h$  [see Fig. 1(d)], similar to observations in fully phase-coherent metal wires [44] and quasi-1D silicon MOSFETs [31,32]. On the other hand, at  $T = 4.2 \text{ K}$  we find  $l_\varphi \simeq 20 \text{ nm}$ , which approaches the length scale of the carrier mean free path  $l \simeq 6 \text{ nm}$  [8]. This therefore indicates the onset of semiclassical conduction, confirmed by the observation that both UCF and weak localization effects subside around this temperature.

It can be shown theoretically [17–19] that both a sufficiently large change in the Fermi energy  $E_F$  and large enough magnetic flux can be regarded as equivalent to a complete change in a sample's disorder configuration. This consequently allows us to study UCF as a function of both gate voltage and magnetic fields. To further test the conductance fingerprint for reproducibility upon thermal cycling, we measured their magnetic field dependence in a separate cooldown.

The conductance at varying magnetic field strengths is plotted in Fig. 2(a) [45]. Importantly, we find that the conductance fluctuations are highly reproducible with minor

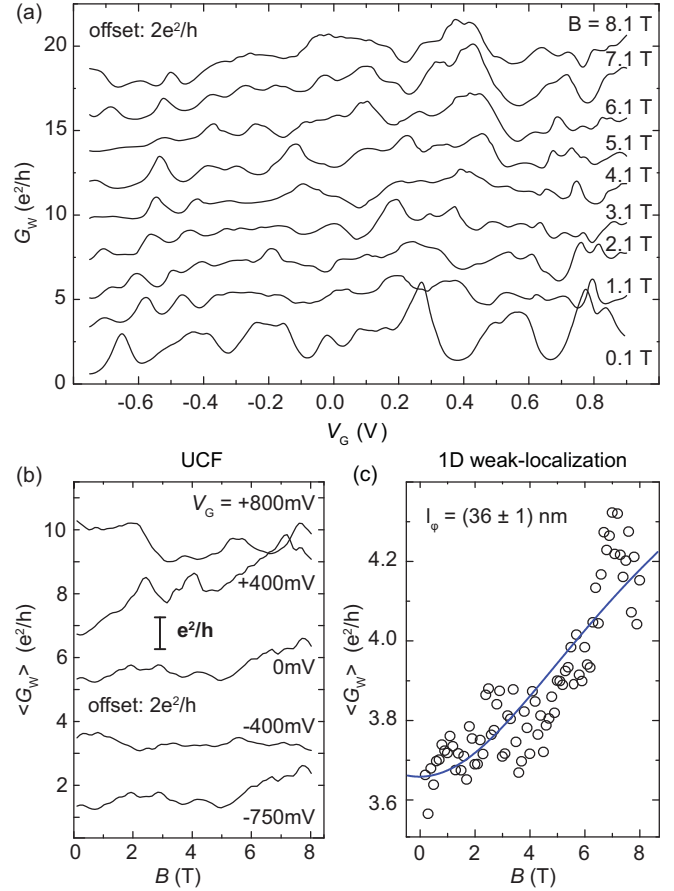


FIG. 2. Magnetotransport at millikelvin temperatures. (a) Gate-voltage-dependent conductance fluctuations for perpendicular magnetic fields between 0.1 and 8.1 T. (b) Magnetoconductance fluctuations for constant gate voltages as indicated in the figure. Individual traces in (a) and (b) have each been offset by  $2e^2/h$ . (c) Mean conductance  $\langle G_W \rangle(B)$ , extracted from traces such as shown in (a), with finer magnetic field increments. The solid blue line shows a fit to Altshuler-Aronov theory [19,43] for 1D weak localization correction [Eq (8)].

changes in the UCF pattern after thermal cycling. We explain this by the robust disorder potential in Si:P wires which is dominated by the position and density of P donor ions providing both charge confinement and scatters for mobile charge [2,8]. However, as we can see from Fig. 2(a), the pattern of the UCF can be sufficiently randomized by the application of a perpendicular magnetic field. Correspondingly, in Fig. 2(b) we plot magnetoconductance at different gate voltages. These data—similar to the gate-voltage fluctuations—also show amplitudes of  $\sim e^2/h$ , as expected from UCF theory [17–19].

A perpendicular magnetic field breaks time-reversal symmetry [19], leading to a gradual quenching of the weak localization contribution. This is illustrated in Fig. 2(c), where we plot the mean conductance  $\langle G_W \rangle$  as a function of magnetic field. The data have been extracted from curves such as those plotted in Fig. 2(a) with finer magnetic field increments. The solid blue line is a fit to the well-known Altshuler and Aronov

[19,43] expression for 1D weak localization:

$$\begin{aligned} \langle G_W(B) \rangle &= G_0 + \delta G_{WL}(B) \\ &= \langle G_W(B \gg B_C) \rangle - g_s g_v \frac{e^2}{h} \frac{1}{L} \left[ \frac{1}{l_\varphi^2} + \frac{e^2 B^2 w^2}{3 \hbar^2} \right]^{-1/2}. \end{aligned} \quad (8)$$

Again assuming  $\alpha g_v = 1$  due to strong intervalley scattering, we find

$$l_\varphi(T \simeq 200 \text{ mK}) = (36 \pm 1) \text{ nm}, \quad (9)$$

in good agreement with the previous extrapolation of  $l_\varphi$  at this temperature. We calculate the critical field [19,43]

$$B_C = \frac{\hbar \sqrt{3}}{e w l_\varphi} \quad (10)$$

at which time-reversal symmetry is broken by enclosing a magnetic flux as large as  $B_C \simeq 5 \text{ T}$ , a direct consequence of the atomic-scale width of the wire, which—due to its atomic dimensions—requires extraordinary large magnetic fields in order to enclose a single magnetic flux quantum  $\Phi_0 = h/e$  within its area  $S = l_\varphi w$ . This confirms that transport along the wire can be regarded as fully phase coherent ( $l_\varphi \simeq L$ ) at  $\simeq 200 \text{ mK}$ . From the fit, we furthermore find  $G_0 = 5.1 e^2/h$ , close to the measured value at 4.2 K and at zero gate voltage,

indicating that both magnetic field and temperature effectively quench the 1D weak localization.

We conclude that electron transport in atomic-scale Si:P wires can be described consistently within the framework of coherent diffusive conduction in quasi-1D metals. We have shown that both the weak localization correction and the amplitude of universal conductance fluctuations reach their universal values at millikelvin temperatures. This confirms that carriers maintain their phase coherence over the length of the wire. As the temperature is raised above 4.2 K, we observe the quantum-coherent to semiclassical transition as Nyquist scattering of electrons causes decoherence over length scales approaching the carrier mean free path. The concomitant disappearance of both UCF and weak localization effects at temperatures above  $T \sim 4.2 \text{ K}$  implies that electron transport in these quasi-1D metals can be well approximated by semiclassical models [2,8] at such low temperatures. Our results thus ultimately confirm that universal concepts of mesoscopic physics such as UCF and weak localization retain their validity in these metallic conductors at the atomic scale.

This research was conducted by the Australian Research Council Centre of Excellence for Quantum Computation and Communication Technology (Project No. CE110001027) and the U.S. National Security Agency and the U.S. Army Research Office under Contract No. W911NF-08-1-0527. M.Y.S. acknowledges an ARC Laureate Fellowship, B.W. acknowledges an ARC DECRA fellowship (Project No. DE160101334).

- 
- [1] S. R. Schofield, N. J. Curson, M. Y. Simmons, F. J. Ruess, T. Hallam, L. Oberbeck, and R. G. Clark, *Phys. Rev. Lett.* **91**, 136104 (2003).
- [2] B. Weber, S. Mahapatra, H. Ryu, S. Lee, A. Fuhrer, T. C. G. Reusch, D. L. Thompson, W. C. T. Lee, G. Klimeck, L. C. L. Hollenberg, and M. Y. Simmons, *Science* **335**, 64 (2012).
- [3] M. Fuechsle, J. A. Miwa, S. Mahapatra, H. Ryu, S. Lee, O. Warschkow, L. C. L. Hollenberg, G. Klimeck, and M. Y. Simmons, *Nat. Nanotechnol.* **7**, 242 (2012).
- [4] B. Weber, Y. H. M. Tan, S. Mahapatra, T. F. Watson, H. Ryu, R. Rahman, L. C. L. Hollenberg, G. Klimeck, and M. Y. Simmons, *Nat. Nanotechnol.* **9**, 430 (2014).
- [5] B. E. Kane, *Nature (London)* **393**, 133 (1998).
- [6] L. C. L. Hollenberg, A. D. Greentree, A. G. Fowler, and C. J. Wellard, *Phys. Rev. B* **74**, 045311 (2006).
- [7] C. D. Hill, E. Peretz, S. J. Hile, M. G. House, M. Fuechsle, S. Rogge, M. Y. Simmons, and L. C. L. Hollenberg, *Sci. Adv.* **1**, e1500707 (2015).
- [8] B. Weber, H. Ryu, Y.-H. M. Tan, G. Klimeck, and M. Y. Simmons, *Phys. Rev. Lett.* **113**, 246802 (2014).
- [9] T. F. Watson, B. Weber, J. A. Miwa, S. Mahapatra, R. M. P. Heijnen, and M. Y. Simmons, *Nano Lett.* **14**, 1830 (2014).
- [10] M. G. House, T. Kobayashi, B. Weber, S. J. Hile, T. F. Watson, J. van der Heijden, S. Rogge, and M. Y. Simmons, *Nat. Commun.* **6**, 8848 (2015).
- [11] T. F. Watson, B. Weber, M. G. House, H. Büch, and M. Y. Simmons, *Phys. Rev. Lett.* **115**, 166806 (2015).
- [12] D. K. Ferry, *Science* **335**, 45 (2012).
- [13] P. W. Anderson, *Phys. Rev.* **109**, 1492 (1958).
- [14] C. W. J. Beenakker, *Rev. Mod. Phys.* **69**, 731 (1997).
- [15] A. Dusko, A. Saraiva, and B. Koiller, [arXiv:1603.06936](https://arxiv.org/abs/1603.06936).
- [16] J. S. Smith, D. W. Drumm, A. Budi, J. A. Vaitkus, J. H. Cole, and S. P. Russo, *Phys. Rev. B* **92**, 235420 (2015).
- [17] B. L. Altshuler, V. E. Kravtsov, and I. V. Lerner, *JETP Lett.* **43**, 441 (1986).
- [18] P. A. Lee, A. D. Stone, and H. Fukuyama, *Phys. Rev. B* **35**, 1039 (1987).
- [19] C. W. J. Beenakker and H. v. Houten, *Solid State Phys.* **44**, 1 (1991).
- [20] All conductance data have been corrected for a constant series resistance of  $R_s = 2 \text{ k}\Omega$  arising from the 2D  $\delta$ -doped banks which connect to the  $S$  and  $D$  contacts, as detailed in Ref. [8].
- [21] K. E. J. Goh, L. Oberbeck, M. Y. Simmons, A. R. Hamilton, and M. J. Butcher, *Phys. Rev. B* **73**, 035401 (2006).
- [22] S. R. McKibbin, W. R. Clarke, and M. Y. Simmons, *Physica E* **42**, 1180 (2009).
- [23] N. F. Mott and W. D. Twose, *Adv. Phys.* **10**, 107 (1961).
- [24] M. Cahay, M. McLennan, and S. Datta, *Phys. Rev. B* **37**, 10125 (1988).
- [25] S. Datta, *Electronic Transport in Mesoscopic Systems*, Cambridge Studies in Semiconductor Physics and Microelectronic Engineering (Cambridge University Press, Cambridge, U.K., 1995).

- [26] C. W. J. Beenakker and H. van Houten, *Phys. Rev. B* **37**, 6544 (1988).
- [27] P. A. Lee and T. V. Ramakrishnan, *Rev. Mod. Phys.* **57**, 287 (1985).
- [28] We estimate  $l_T = 57$  nm at  $T = 4.2$  K and  $l_T \sim 262$  nm at 200 mK based on the diffusion constant  $D = \frac{1}{2} \frac{\hbar}{m^*} k_F l = 1.8 \times 10^{-3}$  m<sup>2</sup>/s.
- [29] H. Fukuyama, *Surf. Sci.* **113**, 489 (1982).
- [30] G. Qian, Y.-C. Chang, and J. R. Tucker, *Phys. Rev. B* **71**, 045309 (2005).
- [31] W. J. Skocpol, P. M. Mankiewich, R. E. Howard, L. D. Jackel, D. M. Tennant, and A. D. Stone, *Phys. Rev. Lett.* **56**, 2865 (1986).
- [32] W. J. Skocpol, *Phys. Scr.* **T19A**, 95 (1987).
- [33] Different valleys are sufficiently mixed [29,46] if  $1/\tau_v \gg 1/\tau_\varphi$ , where  $\tau_v$  is the intervalley and  $\tau_\varphi = l_\varphi^2/D$  the inelastic scattering rate, respectively. In this case,  $\alpha = 1/g_v$ . In high-density  $\delta$ -doped Hall bars [21,47,48] and STM-patterned wires [41,48],  $\alpha g_v \approx 1$  is usually found due to the high Coulomb scattering rate with P ions,  $1/\tau \sim 10^{14}$ /s [21], exceeding  $1/\tau_\varphi \sim 10^{12}$ /s by two orders of magnitude.
- [34] J. F. Lin, J. P. Bird, L. Rotkina, and P. A. Bennett, *Appl. Phys. Lett.* **82**, 802 (2003).
- [35] J. J. Lin and N. Giordano, *Phys. Rev. B* **33**, 1519 (1986).
- [36] S. Wind, M. J. Rooks, V. Chandrasekhar, and D. E. Prober, *Phys. Rev. Lett.* **57**, 633 (1986).
- [37] D. Natelson, R. L. Willett, K. W. West, and L. N. Pfeiffer, *Phys. Rev. Lett.* **86**, 1821 (2001).
- [38] C. Schonenberger, A. Bachtold, C. Strunk, J. P. Salvetat, and L. Forro, *Appl. Phys. A* **69**, 283 (1999).
- [39] R. G. Wheeler, K. K. Choi, A. Goel, R. Wisnieff, and D. E. Prober, *Phys. Rev. Lett.* **49**, 1674 (1982).
- [40] D. M. Pooke, N. Paquin, M. Pepper, and A. Gundlach, *J. Phys.: Condens. Matter* **1**, 3289 (1989).
- [41] F. J. Ruess, B. Weber, K. E. J. Goh, O. Klochan, A. R. Hamilton, and M. Y. Simmons, *Phys. Rev. B* **76**, 085403 (2007).
- [42] B. L. Altshuler, A. G. Aronov, and D. E. Khmel'nitsky, *J. Phys. C* **15**, 7367 (1982).
- [43] B. Altshuler and A. Aronov, *JETP Lett.* **33**, 498 (1981).
- [44] A. Benoit, C. P. Umbach, R. B. Laibowitz, and R. A. Webb, *Phys. Rev. Lett.* **58**, 2343 (1987).
- [45] A small field of 100 mT was applied to quench superconductivity at zero magnetic field in the aluminum Ohmic contacts.
- [46] T. Ando, A. B. Fowler, and F. Stern, *Rev. Mod. Phys.* **54**, 437 (1982).
- [47] S. Agan, O. A. Mironov, E. H. C. Parker, T. E. Whall, C. P. Parry, V. Y. Kashirin, Y. F. Komnik, V. B. Krasovitsky, and C. J. Emeleus, *Phys. Rev. B* **63**, 075402 (2001).
- [48] S. J. Robinson, J. S. Kline, H. J. Wheelwright, J. R. Tucker, C. L. Yang, R. R. Du, B. E. Volland, I. W. Rangelow, and T. C. Shen, *Phys. Rev. B* **74**, 153311 (2006).